Reduced relative intensity noise of a coherently combined single-mode semiconductor laser array under injection locking

Xu Ke, Bing Xiong,* Changzheng Sun, Yi Luo,† Weichao Ma, Zhibiao Hao, Yanjun Han, Jian Wang, Lai Wang, and Hongtao Li

Beijing National Research Center for Information Science and Technology, Department of Electronic Engineering, Tsinghua University, Beijing 100084, People's Republic of China

(Received 24 June 2018; revised manuscript received 9 October 2018; published 14 November 2018)

A scheme for reducing the relative intensity noise (RIN) of laser source by an injection locked single-mode semiconductor laser array is proposed and demonstrated. Intensity and phase noise of the slave laser under injection locking are first analyzed by rate equations, and the RIN of the injection locked laser array after coherent combining is then estimated. The RIN of the injection-locked N-element laser array can be reduced by a factor about $1/N$ over the entire frequency range in the ideal case. Measurements with a two-element distributed feedback laser array confirm the main theoretical predictions and a nearly 3 dB reduction in RIN is obtained. The effect of the key parameters on the RIN of the injection locked array is investigated as well.

DOI: 10.1103/PhysRevA.98.053824

I. INTRODUCTION

Semiconductor lasers have been widely used in many fields such as fiber communications, imaging, solid-state laser pump, etc., due to their excellent reliability, high efficiency, and ease for integration [1]. In particular, semiconductor lasers with low relative intensity noise (RIN) are required in microwave photonics such as microwave fiber-optic links, radar, and electronic warfare [2,3]. There are four major approaches to reducing the RIN of semiconductor lasers. The first is to increase the output power while keeping single-mode operation [3–7]. However, due to the nonlinear effects such as spatial hole burning, the maximum output power is limited, thus limiting the lowest attainable RIN. The second one is to switch semiconductor lasers from class B to class A by increasing the photon lifetime, so as to suppress the relaxation oscillation induced RIN peak [8,9]. However, the improvement in RIN achievable with this method is limited due to the relatively low output power. The third technology is by strong injection locking, which enhances the relaxation oscillation frequency and suppresses the relaxation oscillation peak of the injection locked laser, thus reducing its RIN [10,11]. But the requirement of a high power and low RIN master laser limits its practical use. The last one is through fiber transmission [12]. The fiber dispersion broadens the intensity fluctuation in the time domain, resulting in a suppressed relaxation oscillation peak in the frequency domain. However, usually several kilometers of fiber have to be used, which limits its application. To satisfy the requirement of the next generation microwave photon links, a new method for reducing the RIN of semiconductor lasers is needed, which should be compatible with existing technologies.

The RIN of a single semiconductor is given by [1]

$$R_{\text{single}} = \frac{2S_{\delta P}(\omega)}{P_0^2}, \tag{1}$$

where P_0 is the average output power and $S_{\delta P}(\omega)$ is the double-sided noise spectral density. For an N-element laser array with coherent output but uncorrelated noise from each array element, the RIN of the coherently combined array (CCA) would be

$$R_{CCA} = \frac{1}{(NP_0)^2}\sum_{i=1}^{N} 2S_{\delta P_i}(\omega) = \frac{1}{N}\frac{2S_{\delta P(\omega)}}{{P_0}^2} = \frac{1}{N}R_{\text{single}}, \tag{2}$$

which is reduced by a factor about $1/N$ of a single laser.

Here, we propose a scheme with an N-element semiconductor laser array to realize RIN improvement along with the above idea, as shown in Fig. 1. To ensure coherent operation of the array, the lasers are injection locked by a master laser. The slave lasers are isolated from each other, the light from the master laser is used to injection lock each laser in the array by way of a beam splitter, and the output of the slave lasers are combined by the output coupler.

Different from the RIN reduction by strong injection locking, the injection ratio of the scheme here is relatively low and its influence on the relaxation oscillation can be neglected. Actually, the noises of the slave lasers are not completely uncorrelated, as they are injection locked to the same master laser. The noise correlation between the slave lasers is influenced by the injection ratio and phase difference between the master and the slave lasers. Moreover, the combining phase and coupling delay may result in conversion of phase noise into intensity noise and noise beat.

To make this technology applicable, the influence of these issues needs to be analyzed. In this paper, we present a detailed investigation on the RIN characteristics of the proposed

*bxiong@tsinghua.edu.cn
†luoy@tsinghua.edu.cn

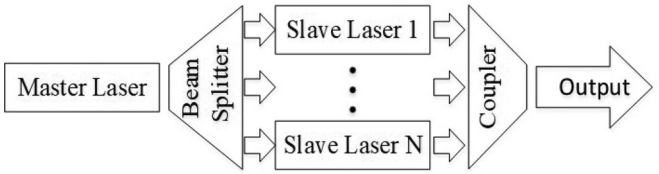

FIG. 1. Scheme diagram of combined injection locking array for low RIN source.

scheme by adopting an analytic model that takes into account both the zero-point noise and the master laser noise. The theoretical model is detailed in Sec. II. The intensity and phase noise of a single slave laser under injection locking is first discussed. The RIN performance of a coherently combined N-element laser array under injection locking is then investigated. Here, we emphasize that we are concerned with the behavior of slave lasers under stable injection locking, and nonlinear dynamics such as chaos or synchronization [13] are not the concern of this work. Simulation results based on this theoretical model are presented in Sec. III, where the RIN and frequency (phase) noise of a single laser under injection locking is analyzed and used to calculate the change in the RIN that occurs after coherent combining. In Sec. IV, measurements with a two-element distributed feedback laser (DFB) array confirm the main theoretical predictions.

II. THEORETICAL MODEL

In this work, the intensity and phase noise of a single slave laser under injection locking is obtained with rate equations and small signal analysis. Different from the analysis in Ref. [14], the correlation between the injected photon density and the phase fluctuation is considered here.

A. Noise model of a single semiconductor laser under injection locking

Because of the quantum nature of spontaneous emission, the description of semiconductor laser noise normally requires a quantum-mechanical formulation of rate equations [15]. Nevertheless, the RIN of an injection-locked laser can be adequately modeled by the classical phenomenological rate equations with spontaneous radiation and Langevin noise sources [14,16–18],

$$\begin{aligned}\frac{dS}{dt} &= \Gamma A(1-k_sS)(n-n_{tr})S - \frac{S}{\tau_{ph}} + \Gamma\beta R_{sp} \\ &\quad + 2\kappa\sqrt{S_{inj}S}\cos(\phi-\phi_{inj}) + F_s, \\ \frac{d\phi}{dt} &= \frac{\alpha}{2}\left[\Gamma A(1-k_sS)(n-n_{tr}) - \frac{1}{\tau_p}\right] \\ &\quad - \kappa\sqrt{\frac{S_{inj}}{S}}\sin(\phi-\phi_{inj}) - \Delta\omega_{inj} + F_\phi, \\ \frac{dn}{dt} &= \frac{I}{qV} - \frac{n}{\tau_e} - A(1-k_sS)(n-n_{tr})S + F_n,\end{aligned} \tag{3}$$

where S, ϕ, and n are photon number density, phase, and carrier density in the laser cavity under optical injection. S_{inj} and ϕ_{inj} are the photon number density and phase of the injected light. $\Delta\omega_{inj} = \omega_{inj} - \omega_{fr}$ is the detuning frequency. F_s, F_ϕ, and F_n are the Langevin noise sources for photon, phase, and carrier, respectively. The description of the other parameters is shown in Table I.

TABLE I. Description of the parameters.

Symbol	Description
α	Linewidth-enhancement factor
A	Gain coefficient
Γ	Optical confinement factor
k_s	Gain compression factor
n_{tr}	Transparent carrier density
β	Spontaneous emission factor
V	Active volume
τ_{ph}	Photon lifetime
τ_e	Carrier lifetime
κ	Coupling rate
R	Power reflectivity of the laser facets

Small variations δS, $\delta\phi$, δn, δS_{inj}, and $\delta\phi_{inj}$ about the stable injection-locked operating point S_0, ϕ_0, n_0, S_{inj}, and ϕ_{inj} are described as follows [14]:

$$\begin{aligned}&\begin{bmatrix} j\omega+m_{ss} & m_{s\phi} & m_{sn} \\ m_{\phi s} & j\omega+m_{\phi\phi} & m_{\phi n} \\ m_{ns} & 0 & j\omega+m_{nn}\end{bmatrix}\begin{bmatrix}\delta S(\omega)\\ \delta\phi(\omega)\\ \delta n(\omega)\end{bmatrix} \\ &\quad = \begin{bmatrix} m_{si}\\ m_{\phi i}\\ 0\end{bmatrix}\delta S_{inj}(\omega) + \begin{bmatrix} m_{s\phi}\\ m_{\phi\phi}\\ 0\end{bmatrix}\delta\phi_{inj}(\omega) + \begin{bmatrix} F_s\\ F_\phi\\ F_n\end{bmatrix},\end{aligned} \tag{4}$$

where m_{ij} depends on the stationary state parameters, which are shown in Appendix A. The photon density fluctuation δS and phase fluctuation $\delta\phi$ are derived as

$$\begin{aligned}\delta Q(\omega) &= H_{Qsi}(\omega)\delta S_{inj}(\omega) + H_{Q\phi i}(\omega)\delta\phi_{inj}(\omega) \\ &\quad + H_{Qs}(\omega)F_s + H_{Q\phi}(\omega)F_\phi + H_{Qn}(\omega)F_n,\end{aligned} \tag{5}$$

where $Q = S, \phi$ and the transfer functions such as $H_{Qsi}(\omega)$ are given in Appendix B. According to the Wiener-Khinchin theorem, the spectrum density of δS and $\delta\phi$ are

$$\begin{aligned}&\langle|\delta Q(\omega)|^2\rangle \\ &\quad = |H_{Qsi}(\omega)|^2\langle|\delta S_{inj}|^2\rangle + |H_{Q\phi i}(\omega)|^2\langle|\delta\phi_{inj}|^2\rangle \\ &\qquad + 2\,\mathrm{Re}\{H_{Qsi}(\omega)H^*_{Q\phi i}(\omega)\langle\delta S_{inj}(\omega)\delta\phi_{inj}(\omega)\rangle\} \\ &\qquad + |H_{Q\phi}(\omega)|^2\langle F_\phi F_\phi\rangle + |H_{Qs}(\omega)|^2\langle F_sF_s\rangle \\ &\qquad + |H_{Qn}(\omega)|^2\langle F_nF_n\rangle + 2\,\mathrm{Re}\{H_{Qs}(\omega)H^*_{Qn}\langle F_sF_n\rangle\},\end{aligned} \tag{6}$$

where $\langle AB\rangle$ denotes the spectrum density of the correlation between noises A and B. The first three terms of (6) are correlated with the master laser and the other terms are related to the slave laser. Although the phase noise has no direct effect on the RIN of a laser, the phase noise will be converted to intensity noise of the laser array output. So the phase noise of the slave laser is analyzed here as well.

The phase fluctuation between the internal and external cavity can be neglected, but the difference of the intensity fluctuation should be considered [19]. The injected photon density fluctuation δS_{inj} involves external light fluctuation and

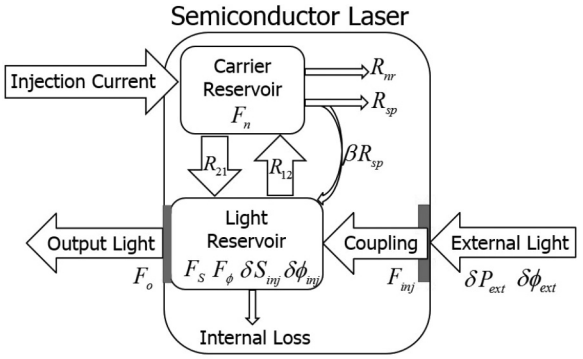

FIG. 2. Noise model diagram for injection locking. F_{inj} and F_o are the zero-point noise induced by the injection facet and the output facet, respectively. δP_{ext} and $\delta\phi_{\text{ext}}$ are the power and phase fluctuation of the external injected light. The gray blocks represent equivalent mirrors.

zero-point noise from the input facet,

$$\delta S_{inj} = \frac{S_{inj}}{P_{inj}}[(1-R)\delta P_{\text{ext}} + F_{inj}], \tag{7}$$

where P_{inj} is the injected power. Then the correlation functions of injected light in (6) are

$$\langle \delta S_{inj}(\omega)^2\rangle = \left(\frac{S_{inj}}{P_{inj}}\right)^2 [(1-R)^2\langle|\delta P_{\text{ext}}(\omega)|^2\rangle + \langle F_{inj}F_{inj}\rangle + 2(1-R)\langle F_{inj}\delta P_{\text{ext}}(\omega)\rangle], \tag{8}$$

$$\langle|\delta\phi_{inj}(\omega)|^2\rangle = \langle|\delta\phi_m(\omega)|^2\rangle, \tag{9}$$

$$\langle \delta S_{inj}(\omega)\delta\phi_{inj}(\omega)\rangle = \frac{S_{inj}}{P_{inj}}(1-R)\left(\frac{1}{2}h\nu\upsilon_g\alpha_m V/\Gamma\right) \times 10^{\frac{Att}{10}}\langle \delta S_m(\omega)\delta\phi_m(\omega)\rangle, \tag{10}$$

where the subscript "m" in (9) and (10) denotes the master laser. δS_m and $\delta\phi_m$ can be derived by setting coupling coefficient $\kappa = 0$ in (5). h, υ_g, α_m, and ν are Planck constant, group velocity, mirror coupling loss, and light frequency. The injection ratio is adjusted by a variable optical attenuator, which has an attenuation given by Att and introduces no excess noise. The particle flows in the injection locking system, as required by the Langevin method, are shown in Fig. 2. The other correlation functions in (6) are derived in Appendix C. Compared with Ref. [14], the main difference here is that the correlation between the injected photon density and the phase fluctuation represented by (10) is not zero, but depends on the master laser.

B. RIN model of the coherently combined array

Next we consider the case of coherent combining of an N-element array injection locked to the same master laser. The output electric field of each slave laser can be written as $E_p(t) = \sqrt{S_p(t)}\exp[\phi_p(t)]$, for $p = 1$ to N. The field of the combined beam is given by

$$E_T(t) = A\sum_{p=1}^{N}\sqrt{S_p(t-\tau_p)}\exp[\phi_p(t-\tau_p)], \tag{11}$$

where A is the complex coefficient of the coupler and τ_p is the coupling delay. The intensity of the combined light in time domain is

$$S_T(t) = |A|^2\sum_{p=1}^{N}S_p(t-\tau_p) + 2|A|^2 \times\sum_{p<q}\sqrt{S_p(t-\tau_p)S_q(t-\tau_q)} \times\cos[\phi_p(t-\tau_p)-\phi_q(t-\tau_q)], \tag{12}$$

where $\phi_p(t-\tau_p)-\phi_q(t-\tau_q)$ is the phase difference between two array elements. Similar to the process mentioned above, the light intensity fluctuation δS_T can be derived by small-signal analysis, with the transfer functions shown in Appendix D:

$$\delta S_T(\omega) = \sum_{p=1}^{N}H_{Ts}^{p}(\omega)\delta S_{o_p}(\omega) + \sum_{p=1}^{N}H_{T\phi}^{p}(\omega)\delta\phi_p(\omega). \tag{13}$$

The fluctuation of photon density noise is given by

$$\delta S_{o_p}(\omega) = \delta S_p(\omega) + F_{o_p}\big/\left(\tfrac{1}{2}h\nu\upsilon_g\alpha_m V_p/\Gamma_p\right), \tag{14}$$

where F_{o_p} is the zero-point noise. We obtain the spectrum density of $\delta S_T(\omega)$ as

$$\langle|\delta S_T(\omega)|^2\rangle = \sum_{p=1}^{N}\left|H_{Ts}^{p}(\omega)\right|^2\left\langle\left|\delta S_{o_p}(\omega)\right|^2\right\rangle + \sum_{p=1}^{N}\left|H_{T\phi}^{p}(\omega)\right|^2\langle|\delta\phi_p(\omega)|^2\rangle + 2\,\text{Re}\left\{\sum_{1\leqslant p<q\leqslant N}H_{Ts}^{p}(\omega)H_{Ts}^{q\,*}(\omega)\left\langle\delta S_{o_p}(\omega)\delta S_{o_q}(\omega)\right\rangle\right\} + 2\,\text{Re}\left\{\sum_{1\leqslant p<q\leqslant N}H_{T\phi}^{p}(\omega)H_{T\phi}^{q\,*}(\omega)\langle\delta\phi_p(\omega)\delta\phi_q(\omega)\rangle\right\} + 2\,\text{Re}\left\{\sum_{p,q=1}^{N}H_{Ts}^{p}(\omega)H_{T\phi}^{q\,*}(\omega)\left\langle\delta S_{o_p}(\omega)\delta\phi_q(\omega)\right\rangle\right\}. \tag{15}$$

According to (5) and (14) we can derive the correlation function in (15) as shown in Appendix E. The average light intensity is given by

$$S_{TN}(t) = |A|^2\left[\sum_{p=1}^{N}S_p + 2\sum_{p<q}\sqrt{S_pS_q}\cos(\phi_p-\phi_q)\right]. \tag{16}$$

Consequently, the total RIN of the semiconductor laser array under injection locking is

$$R_{TN} = \frac{2\langle|\delta S_{TN}(\omega)|^2\rangle}{S_{TN}(t)^2}. \tag{17}$$

III. SIMULATION RESULTS

The injected light of the master laser not only affects the noise characteristics of each slave laser, but induces additional noise in the combined output. Actually, the injected noise δS_{inj} and $\delta\phi_{inj}$ induce noise correlation among the slave lasers, thus affecting the RIN of the laser array. We will analyze their contributions in stable locking range [20]. In Sec. III A and Sec. III B, we focus on the effect of the master laser on the RIN and frequency (phase) noise characteristics of the slave laser, which is important for our scheme, but ignored in the previous study [14,16–18]. Then the RIN of the array in the ideal case, i.e., zero combining phase and equal coupling delay, is analyzed in Sec. III C. For nonideal combining, the effect of combining phase and coupling delay on the RIN of the array is analyzed in Sec. III D. For simplicity, the parameters of the master and the slave lasers are taken to be the same in our simulations. We set $\alpha = 5$, $A = 1.4 \times 10^{-6}$ cm^3/s, $\Gamma = 0.35$, $k_s = 2 \times 10^{-17}$ cm^3, $n_{tr} = 1.1 \times 10^{18}$ cm^{-3}, $\beta = 1 \times 10^{-5}$, $V = 6 \times 10^{-11}$ cm^3, $\tau_{ph} = 1.75$ ps, $\tau_e = 2$ ns, $\kappa = 89.3$ GHz, and $R = 0.25$.

A. Effect of master laser noise on the RIN of a single slave laser

According to the first three terms in (6), the contribution from the master laser to the RIN includes δS_{inj}, $\delta\phi_{inj}$, and their correlation (may be negative). When compared with δS_{inj} and the correlation, the contribution of $\delta\phi_{inj}$ dominates at low frequencies as shown in Fig. 3(a). The ratio $R_{\delta\phi_{inj}}$ of the contribution of $\delta\phi_{inj}$ to the total noise source is larger than 90% in most cases, except for $\phi - \phi_{inj}$ near zero. Actually, if $\phi - \phi_{inj} = 0^\circ$, there will be no contribution of $\delta\phi_{inj}$.

Different from δS_{inj}, the contribution of $\delta\phi_{inj}$ to the RIN is independent of the injection ratio, but depends on the master laser according to (9). Therefore, when $\phi - \phi_{inj}$ is far from zero, the influence of the injection ratio to the contribution of the master laser can be neglected at low frequencies. It is worth noting that a positive $\phi - \phi_{inj}$ will enhance the contribution from both the master and the slave lasers at low frequencies as shown in Fig. 3(b). Thus the positive $\phi - \phi_{inj}$ should be avoided to reduce the RIN.

Since $\delta\phi_{inj}$ has a significant influence on the RIN characteristics of the laser array in most cases, it would be beneficial to reduce the phase noise of the master laser. As we know, an elevated injection current implies a reduced phase noise within certain limits. We verify this result in Fig. 4 by comparing the RIN obtained with the master laser under different injection currents. Actually, further increasing the injection current of the master laser has relatively insignificant influence on the RIN of the injection locked slave laser, as the main contribution to the RIN comes from the slave laser itself.

B. Effect of spontaneous radiation in slave laser on its frequency noise

According to (15), the phase noise of slave lasers will be converted to the RIN of the laser array in most cases. At high

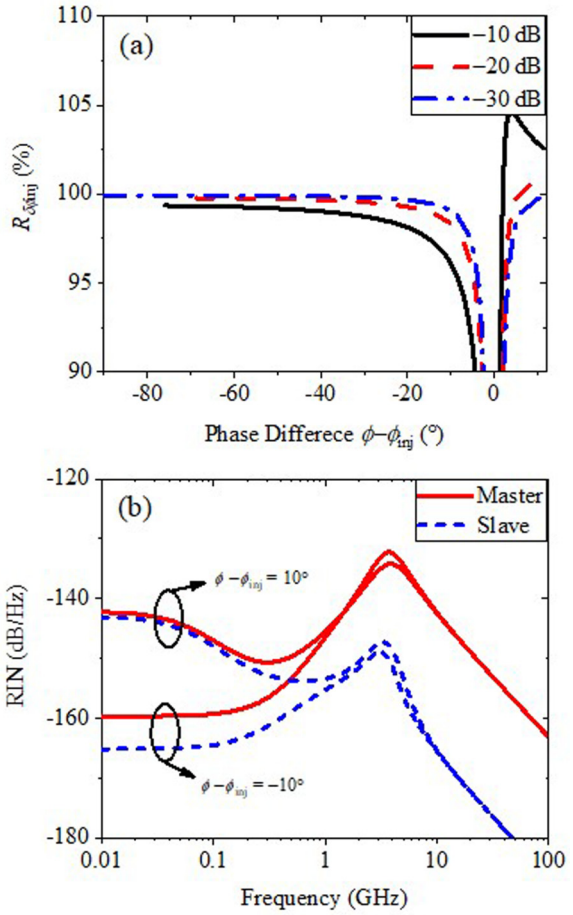

FIG. 3. (a) Ratio of the contribution of $\delta\phi_{inj}$ to the total noise source of the master laser. (b) The contribution of the master and the slave laser noise sources on the RIN at $R_{inj} = -30$ dB.

frequencies, the frequency noise is given by

$$\langle|\delta\dot{\phi}(\omega)|^2\rangle = \omega^2\langle|\delta\phi(\omega)|^2\rangle. \tag{18}$$

Although the frequency noise characteristics with various injection parameters has been analyzed in Ref. [21], the

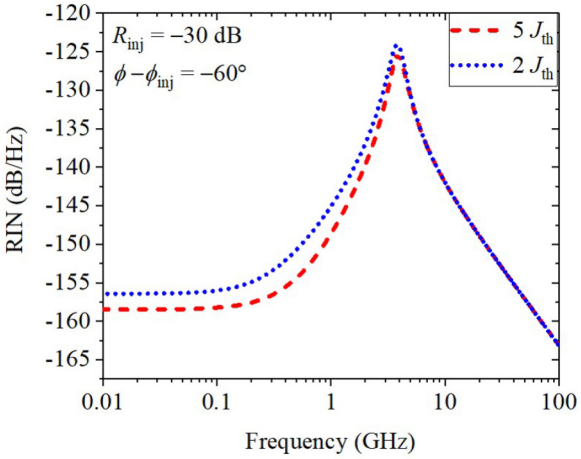

FIG. 4. RIN characteristics under injection locking with different injection currents into the master laser.

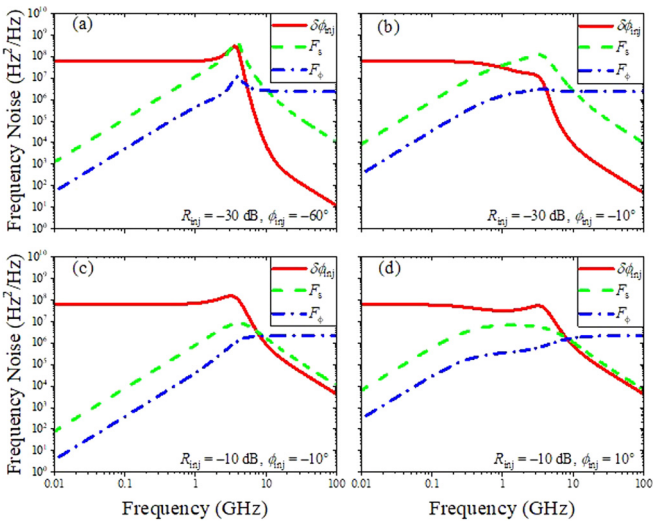

FIG. 5. Main contributions of the noise sources to the frequency noise with different injection parameters, $J = J_m = 2J_{th}$. The symbols F_s, F_ϕ, $\delta\phi_{inj}$ represent their contributions to the frequency noise.

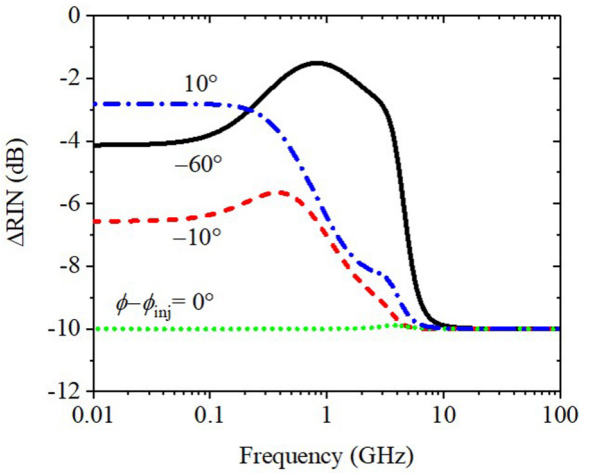

FIG. 6. Variation in RIN between the array ($N = 10$) and a single laser under injection locking at different $\phi - \phi_{inj}$ in the ideal case. $J = J_m = 2J_{th}$; injection ratio is −30 dB.

influence of different noise sources on the frequency noise remains unclear. As confirmed by our simulations, the noise contributions of F_n and δS_{inj} can be neglected compared with F_s, F_ϕ, and $\delta\phi_{inj}$, even at 0 dB injection ratio. Therefore, the approximate frequency noise of the injected laser can be expressed as

$$\langle|\delta\dot{\phi}(\omega)|^2\rangle \approx \omega^2|H_{\phi\phi i}(\omega)|^2\langle|\delta\phi_{inj}(\omega)|^2\rangle + \omega^2|H_{\phi s}(\omega)|^2\langle F_s F_s\rangle + \omega^2|H_{\phi\phi}(\omega)|^2\langle F_\phi F_\phi\rangle. \tag{19}$$

Figure 5 shows the main contributions of the noise sources to the frequency noise with various injection parameters. We find the contributions at low and high frequencies are dominated by the phase fluctuations of the master and slave laser, respectively, i.e., $\delta\phi_{inj}$ and F_ϕ.

We focus on the frequency noise at low frequencies, which may result in the RIN deterioration of the laser array. It is found that light injection helps suppress the contribution of spontaneous radiation in the slave laser (F_s and F_ϕ) to the frequency noise at low frequencies. Comparing Figs. 5(a), 5(b), and 5(c), such suppression becomes more significant for larger negative phase difference $\phi - \phi_{inj}$ and higher injection ratio R_{inj}. However, this suppression is insignificant when $\phi - \phi_{inj}$ is positive, as shown in Fig. 5(d). The suppressed contributions of the slave laser to the frequency noise at low frequencies may explain the linewidth reduction in mutually injection locked lasers [22].

C. RIN improvement of the coherently combined N-element array in the ideal case

Under the ideal combining condition, i.e., equal coupling delay τ_p and zero phase difference $\phi_p - \phi_q$ between the slave lasers, the intensity noise of the injection locked laser array is independent of the phase noise of the slave lasers:

$$\langle|\delta S_T(\omega)|^2\rangle = \sum_{p=1}^{N}|H_{Ts}^{p}(\omega)|^2\langle|\delta S_{o_p}(\omega)|^2\rangle + 2\,\mathrm{Re}\left\{\sum_{1\leqslant p<q\leqslant N} H_{Ts}^{p}(\omega)H_{Ts}^{q\,*}(\omega)\langle\delta S_{o_p}(\omega)\delta S_{o_q}(\omega)\rangle\right\}. \tag{20}$$

The first term is the sum of the intensity noise of all the slave lasers, while the second term is associated with the correlation between different slave lasers due to injection locking. In the absence of correlation, i.e., the second term in (20) being zero, the RIN of the array is $1/N$ of a single laser under injection locking.

The correlation of intensity noise between the different slave lasers comes from the master laser and the contribution of $\delta\phi_{inj}$ is dominant at low frequencies in most cases, as shown in Fig. 3(a). Therefore, alleviating the contribution of $\delta\phi_{inj}$ by eliminating the phase difference between the master and the slave lasers in negative direction can suppress the correlation. This result is verified by the variation in RIN between the array and a single laser under injection locking as shown in Fig. 6. When $\phi - \phi_{inj} = 0^\circ$, the reduction of RIN is nearly 10 dB in the entire frequency range, as a result of the negligible contribution of δS_{inj}.

D. RIN of the coherently combined array in the nonideal case

In a practical case, the combining phase and the coupling delay differences are not exactly zero, and we need to investigate their influences on the RIN performance of the coherently combined light. For the sake of clarity, the case of a two-element laser array is discussed in the following.

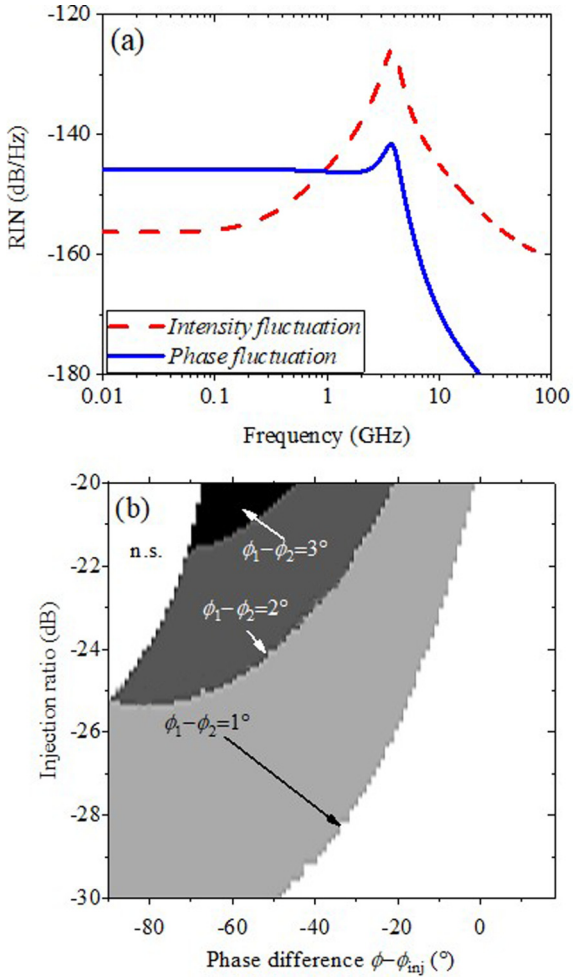

FIG. 7. (a) Noise contributions on the RIN of the array ($N = 2$) with the same coupling delays under different injection parameters. $J = J_m = 2J_{th}$, $\phi_1 - \phi_2 = 5°$, $R_{inj} = -10$ dB, $\phi - \phi_{inj} = -60°$, *Intensity fluctuation*, and *Phase fluctuation* represent the contributions of the intensity and phase fluctuation of the slave lasers to the RIN of the array, respectively. (b) Range of improved RIN, i.e., $\Delta R < 0$, with $\tau = 0$ ps and $J = J_m = 2J_{th}$ (n.s.: unstable portion of the locking range).

First, supposing that the coupling delay difference can be neglected, i.e., $\tau = \tau_1 - \tau_2 = 0$, Eq. (15) can be simplified as

$$\langle|\delta S_T(\omega)|^2\rangle = \left|H^1_{Ts}(\omega)\delta S_{o1}(\omega) + H^2_{Ts}(\omega)\delta S_{o2}(\omega)\right|^2 + \left|H^1_{T\phi}(\omega)\delta\phi_1(\omega) + H^2_{T\phi}(\omega)\delta\phi_2(\omega)\right|^2. \tag{21}$$

The intensity noise of the array contains two parts. One part directly comes from the intensity fluctuation of the slave lasers given by the first term in (21), which is the same with the ideal case in (20). The other part is due to conversion from phase noise. The contributions of these two parts to RIN are shown in Fig. 7(a). The RIN resulting from the former accounts for the behavior at high frequencies, whereas the latter is responsible for the reduction of RIN improvement at low frequencies and should be suppressed. It can be simplified as

$$\begin{aligned}&\left|H^1_{T\phi}(\omega)\delta\phi_1(\omega) + H^2_{T\phi}(\omega)\delta\phi_2(\omega)\right|^2 \\ &\quad= 8|A|^4 {S_0}^2\sin^2(\phi_1-\phi_2)\{|H_{\phi s}(\omega)|^2\langle F_s F_s\rangle \\ &\qquad+ |H_{\phi\phi}(\omega)|^2\langle F_\phi F_\phi\rangle + |H_{\phi n}(\omega)|^2\langle F_n F_n\rangle \\ &\qquad+ 2\,\mathrm{Re}[H_{\phi s}(\omega)H_{\phi n}(\omega)\langle F_s F_n\rangle]\}.\end{aligned} \tag{22}$$

It is interesting to note that the conversion of phase noise to intensity noise at low frequencies is independent of the master laser, but mainly comes from the spontaneous emission in the slave lasers. For a single injection locked laser, large negative phase difference $\phi - \phi_{inj}$ and high injection ratio can suppress the RIN deterioration at low frequencies as shown in Fig. 5. The same trend is true for injection locked laser array, as confirmed by Fig. 7(b).

If the coupling delay difference cannot be neglected, Eq. (15) can be simplified as

$$\begin{aligned}\langle|\delta S_T(\omega)|^2\rangle = &\sum_{p=1}^{2}\left|H^p_{Ts}(\omega)\right|^2\left\langle\left|\delta S_{o_p}(\omega)\right|^2\right\rangle \\ &+\sum_{p=1}^{2}\left|H^p_{T\phi}(\omega)\right|^2\langle|\delta\phi_p(\omega)|^2\rangle \\ &+2\,\mathrm{Re}\left\{H^1_{Ts}(\omega){H^2_{Ts}}^*(\omega)\left\langle\delta S_{o_1(\omega)}\delta S_{o_2}(\omega)\right\rangle\right. \\ &+H^1_{T\phi}(\omega){H^2_{T\phi}}^*(\omega)\langle\delta\phi_1(\omega)\delta\phi_2(\omega)\rangle \\ &+H^1_{Ts}(\omega){H^2_{T\phi}}^*(\omega)\left\langle\delta S_{o_1(\omega)}\delta\phi_2(\omega)\right\rangle \\ &\left.+H^2_{Ts}(\omega){H^1_{T\phi}}^*(\omega)\left\langle\delta S_{o_2(\omega)}\delta\phi_1(\omega)\right\rangle\right\}.\end{aligned} \tag{23}$$

Compared with (21), there is beat noise in the cross correlations between the different lasers as shown in the third term of (23). According to Appendix E, it is induced by the master laser and will enhance the RIN deterioration at low frequencies. Among the contribution of the cross correlations, the cross correlation of phase noise, e.g., $\langle\delta\phi_1(\omega)\delta\phi_2(\omega)\rangle$, dominates. The variation in the RIN of the array with unequal coupling delay is shown in Fig. 8(a). It is found that the high injection ratio and small negative $\phi - \phi_{inj}$ help to suppress the RIN deterioration resulting from an unequal coupling delay, and the cycle of the oscillation is related to the coupling delay, i.e., $\Delta f = 1/\tau$. To improve the RIN of the array over that of a single laser under injection locking, i.e., $\Delta R < 0$, the coupling delay difference, injection ratio, phase difference, and combining phase should be optimized. For simplicity, if we can keep $\phi - \phi_{inj}$ close to zero, the range of improved RIN is shown in Fig. 8(b). It is found that the range of $\Delta R < 0$ is sensitive to the combining phase. The nonzero coupling delay will enhance the deterioration of the RIN at low frequencies further, and more critical control of the combining phase is required to improve the RIN of the array.

From the above discussion, it can be concluded that, for negligible coupling delay difference, large negative phase difference between the master and the slave laser and elevated injection ratio can suppress the RIN deterioration at low frequencies. If the coupling delay difference cannot be neglected, the beat noise will enhance the RIN deterioration and a large negative phase difference is improper. In practical cases, the

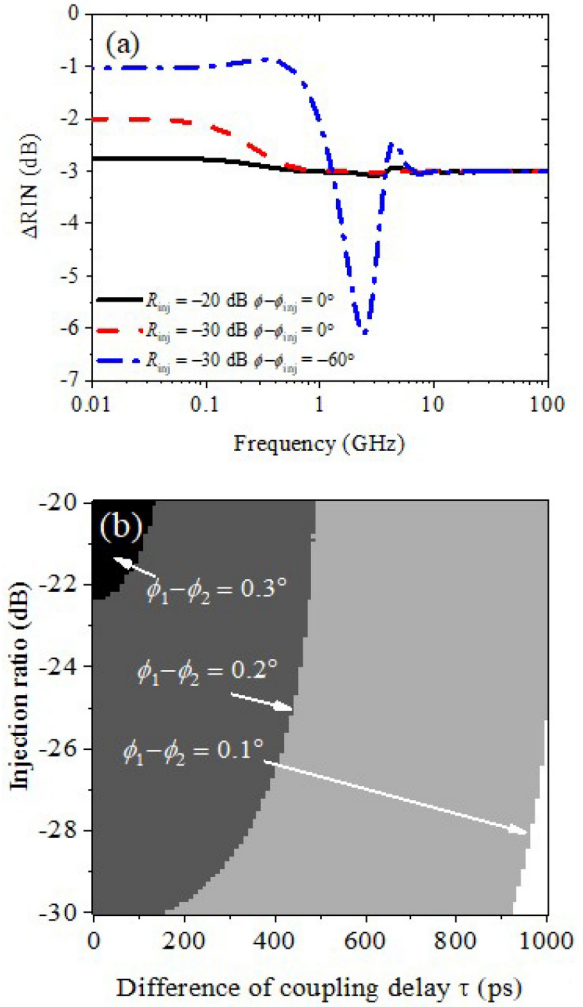

FIG. 8. Effect of unequal coupling delay to RIN, $J = J_m = 2J_{th}$. (a) Variation in RIN between the array ($N = 2$) and a single laser under injection locking with unequal coupling delay, $\phi_1 - \phi_2 = 0.1°$, and $\tau = 200$ ps. (b) Range of improved RIN, $\phi - \phi_{inj} = 0°$.

phase difference should be optimized, and increasing the injection ratio is preferred.

IV. EXPERIMENTAL RESULTS

The RIN performance of a two-element array under injection locking is experimentally investigated to verify the above simulations. In the measurement setup shown in Fig. 9(a), two commercial 1550 nm multiple quantum well (MQW) DFB lasers (DFB1 and DFB2) with no built-in isolators are adopted as the slave lasers, whereas a DFB laser (DFB0) with built-in isolator is used as the master laser. To facilitate injection locking, the wavelength differences between the three lasers are within 0.1 nm. A variable optical attenuator (VOA) is used to adjust the injection ratio. The components in the setup are connected by polarization-maintaining fibers.

As we know, the phase difference $\phi - \phi_{inj} = 0°$ occurs near the maximum negative frequency detuning [14], and the maximum output power corresponds to in-phase combining phase, i.e., $\phi_1 - \phi_2 = 0°$. The difference between the RIN

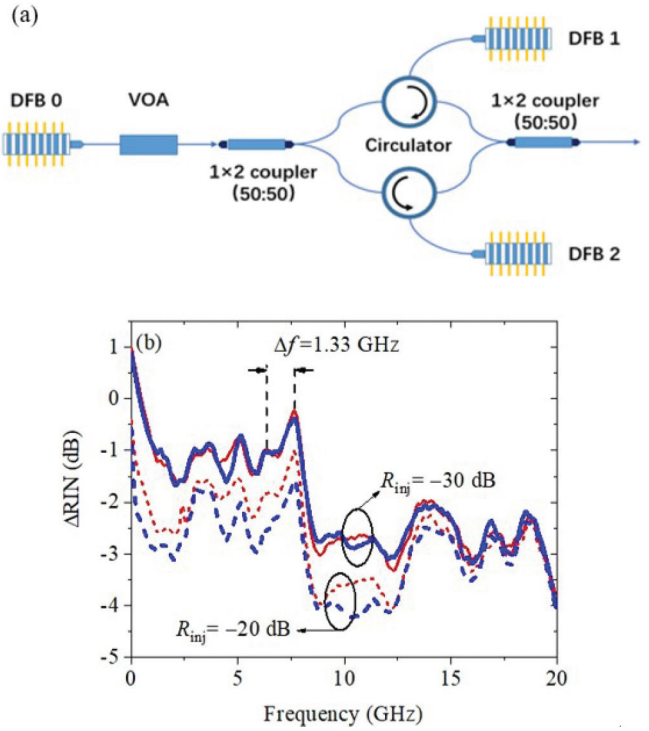

FIG. 9. Experiment results of the variation in RIN of the array ($N = 2$) resulting from the coherent combining with different injection ratio. The heavy and fine lines represent DFB1 and DFB2.

of the array and that of a single slave laser under injection locking is plotted in Fig. 9(b). It is found that the array exhibits a nearly 3 dB RIN reduction and the coupling delay resulting from the unequal fiber length is nearly $1/\Delta f \approx$ 750 ps. As $\phi_1 - \phi_2$ is not exactly zero and the coupling delay cannot be neglected in our experiment, the RIN improvement deteriorates at low frequencies. According to the discussion in Sec. III D, however, increasing the injection ratio can suppress the deterioration, which is in agreement with the experimental result shown in Fig. 9(b).

V. CONCLUSION

We have presented a scheme for RIN improvement by coherently combining a single-mode semiconductor laser array injection locked to a master laser. The RIN characteristics are theoretically investigated based on an analytic model that takes zero-point noise as well as the noise of the master laser into consideration. The contributions of different noise sources to the RIN and frequency noise of a single slave laser are analyzed, and the RIN of an array under ideal and nonideal combining cases are investigated. The main findings can be summarized as follows.

(1) The RIN of the array in the ideal case can be reduced by a ratio of nearly $1/N$ over the entire frequency range. The reduction of the RIN at low frequencies deteriorates due to noise correlation between the slave lasers, which mainly results from the phase noise of the master laser. Keeping the phase difference between the master and the slave lasers close to zero in negative direction and reducing the phase noise of the master laser will suppress this correlation.

(2) When the combining is not ideal, the combining phase and coupling delay differences will result in conversion of phase noise into intensity noise and noise beat at low frequencies. For negligible coupling delay difference, the RIN of the laser array mainly depends on the spontaneous emission of slave lasers. Adopting a higher injection ratio and a larger negative phase difference can suppress this conversion. The nonzero coupling delay difference will enhance the deterioration of the RIN at low frequencies, and more critical control of the combining phase is required to improve the RIN of the array. In practical applications, the coupling delay difference can be reduced to subpicosecond level by adopting an integrated optical coupler, thus relaxing the control requirement for the combining phase.

ACKNOWLEDGMENTS

This work was supported in part by the National Basic Research Program of China (Grant No. 2014CB340002), the High Technology Research and Development Program of China (Grant No. 2015AA017101), Tsinghua University Initiative Scientific Research Program (Grants No. 20131089364, No. 20161080068, and No. 20161080062), and the Open Fund of State Key Laboratory on Integrated Optoelectronics (Grant No. IOSKL2014KF09).

APPENDIX A

$$
\begin{aligned}
m_{ss} &= -\Gamma A(n_0 - n_{tr})(1 - 2k_s S_0) + 1/\tau_{ph} \\
&\quad - \kappa\sqrt{S_{inj}/S_0}\cos(\phi - \phi_{inj}), \\
m_{s\phi} &= 2\kappa\sqrt{S_{inj}S_0}\sin(\phi - \phi_{inj}), \\
m_{sn} &= -\Gamma A(1 - k_s S_0)S_0, \\
m_{\phi s} &= 0.5\alpha\Gamma A(n_0 - n_{tr})k_s - 0.5\kappa\sqrt{S_{inj}/S_0{}^3}\sin(\phi - \phi_{inj}), \\
m_{\phi\phi} &= \kappa\sqrt{S_{inj}/S_0}\cos(\phi - \phi_{inj}), \\
m_{\phi n} &= -0.5\alpha\Gamma A(1 - k_s S_0), \\
m_{ns} &= A(n_0 - n_{tr})(1 - 2k_s S_0), \\
m_{nn} &= 1/\tau_e + A(1 - k_s S_0)S_0, \\
m_{si} &= \kappa\sqrt{S_0/S_{inj}}\cos(\phi - \phi_{inj}), \\
m_{\phi i} &= -0.5\kappa\sqrt{1/(S_0 S_{inj})}\sin(\phi - \phi_{inj}).
\end{aligned}
$$

APPENDIX B

$$
\begin{aligned}
A &= m_{ss} + m_{\phi\phi} + m_{nn}, \\
B &= m_{ss}m_{\phi\phi} + m_{ss}m_{nn} + m_{\phi\phi}m_{nn} \\
&\quad - m_{s\phi}m_{\phi s} - m_{sn}m_{ns}, \\
C &= m_{ss}m_{\phi\phi}m_{nn} + m_{ns}m_{s\phi}m_{\phi n} \\
&\quad - m_{\phi\phi}m_{sn}m_{ns} - m_{nn}m_{s\phi}m_{\phi s}, \\
D &= -j\omega^3 - A\omega^2 + jB\omega + C, \\
H_{ss}(\omega) &= (m_{\phi\phi} + j\omega)(m_{nn} + j\omega)/D, \\
H_{s\phi}(\omega) &= -m_{s\phi}(m_{nn} + j\omega)/D, \\
H_{sn}(\omega) &= (m_{s\phi}m_{\phi n} - m_{sn}m_{\phi\phi} - j\omega m_{sn})/D, \\
H_{ssi}(\omega) &= m_{si}H_{ss}(\omega) + m_{\phi i}H_{s\phi}(\omega), \\
H_{s\phi i}(\omega) &= m_{s\phi}H_{ss}(\omega) + m_{\phi\phi}H_{s\phi}(\omega), \\
H_{\phi s}(\omega) &= (m_{\phi n}m_{ns} - m_{\phi s}m_{nn} - j\omega m_{\phi s})/D, \\
H_{\phi\phi}(\omega) &= [m_{nn}m_{ss} - m_{sn}m_{ns} + i(m_{ss} + m_{nn})]/D - \omega^2/D, \\
H_{\phi n}(\omega) &= (m_{\phi s}m_{sn} - m_{\phi n}m_{ss} - j\omega m_{\phi n})/D, \\
H_{\phi si}(\omega) &= m_{si}H_{\phi s}(\omega) + m_{\phi i}H_{\phi\phi}(\omega), \\
H_{\phi\phi i}(\omega) &= m_{s\phi}H_{\phi s}(\omega) + m_{\phi\phi}H_{\phi\phi}(\omega).
\end{aligned}
$$

APPENDIX C

$$
\begin{aligned}
\langle F_s F_s\rangle &= 2\Gamma\beta R_{sp}S_0 + \frac{2\Gamma^2}{V}\beta R_{sp} \\
&\quad + \frac{2\Gamma^2}{V}\kappa\sqrt{S_{inj}S_0}\cos(\phi_0 - \phi_{inj}), \\
\langle F_\phi F_\phi\rangle &= \langle F_s F_s\rangle/\left(4{S_0}^2\right), \\
\langle F_n F_n\rangle &= \frac{I}{qV^2} + \frac{1}{V}[R_{sp} + R_{nr} + 2\beta R_{sp}S_0 V/\Gamma \\
&\quad - A(1 - k_s S_0)(n_0 - n_{tr})S_0], \\
\langle F_s F_n\rangle &= -\frac{\Gamma}{V}[\beta R_{sp} + 2\beta R_{sp}S_0 V/\Gamma \\
&\quad - A(1 - k_s S_0)(n_0 - n_{tr})S_0], \\
\langle \delta S(\omega)F_o\rangle &= H_{ss}(\omega)\langle F_s F_o\rangle = -H_{ss}(\omega)h\nu P_0, \\
\langle F_o F_o\rangle &= h\nu P_0, \\
\langle F_{inj}F_{inj}\rangle &= h\nu P_{inj}, \\
\langle|\delta P_{\rm ext}(\omega)|^2\rangle &= h\nu P_{inj}/(1 - R) \\
&\quad + 10^{\frac{2Att}{10}}\left(\frac{1}{2}h\nu\upsilon_g\alpha_m V/\Gamma\right)^2\langle|\delta S_m(\omega)|^2\rangle, \\
\langle F_{inj}\delta P_{\rm ext}(\omega)\rangle &= -h\nu P_{inj},
\end{aligned}
$$

where P_0 is the average output power.

APPENDIX D

$$
\begin{aligned}
H^p_{Ts}(\omega) &= |A|^2 e^{-j\omega\tau_p}\left[1 + \sum_{q\neq p}\sqrt{\frac{S_q}{S_p}}\cos(\phi_p - \phi_q)\right], \\
H^p_{T\phi}(\omega) &= -2|A|^2 e^{-j\omega\tau_p}\sum_{q\neq p}\sqrt{S_p S_q}\sin(\phi_p - \phi_q).
\end{aligned}
$$

APPENDIX E

$$
\begin{aligned}
&\langle|\delta S_{o_p}(\omega)|^2\rangle \\
&\quad = \left(\tfrac{1}{2}h\nu\upsilon_g\alpha_m V_p/\Gamma_p\right)^{-2}\langle F_{o_p}F_{o_p}\rangle \\
&\qquad + \langle|\delta S_p(\omega)|^2\rangle + \left(\tfrac{1}{4}h\nu\upsilon_g\alpha_m V_p/\Gamma_p\right)^{-1}\langle\delta S_p(\omega)F_{o_p}\rangle,
\end{aligned}
$$

$$\begin{aligned}
&\langle \delta S_{o_p}(\omega)\delta S_{o_q}(\omega)\rangle \\
&\quad = H^{p}_{ssi}(\omega){H^{q}_{ssi}}^{*}(\omega)\langle \delta S_{inj_p}(\omega)\delta S_{inj_q}(\omega)\rangle \\
&\qquad + H^{p}_{s\phi i}(\omega){H^{q}_{s\phi i}}^{*}(\omega)\langle \delta\phi_{inj_p}(\omega)\delta\phi_{inj_q}(\omega)\rangle \\
&\qquad + H^{p}_{ssi}(\omega){H^{q}_{s\phi i}}^{*}(\omega)\langle \delta S_{inj_p}(\omega)\delta\phi_{inj_q}(\omega)\rangle \\
&\qquad + H^{p}_{s\phi i}(\omega){H^{q}_{ssi}}^{*}(\omega)\langle \delta S_{inj_q}(\omega)\delta\phi_{inj_p}(\omega)\rangle^{*}, \\
&\langle \delta\phi_p(\omega)\delta\phi_q(\omega)\rangle \\
&\quad = H^{p}_{\phi si}(\omega){H^{q}_{\phi si}}^{*}(\omega)\langle \delta S_{inj_p}(\omega)\delta S_{inj_q}(\omega)\rangle \\
&\qquad + H^{p}_{\phi\phi i}(\omega){H^{q}_{\phi\phi i}}^{*}(\omega)\langle \delta\phi_{inj_p}(\omega)\delta\phi_{inj_q}(\omega)\rangle \\
&\qquad + H^{p}_{\phi si}(\omega){H^{q}_{\phi\phi i}}^{*}(\omega)\langle \delta S_{inj_p}(\omega)\delta\phi_{inj_q}(\omega)\rangle \\
&\qquad + H^{p}_{\phi\phi i}(\omega){H^{q}_{\phi si}}^{*}(\omega)\langle \delta S_{inj_q}(\omega)\delta\phi_{inj_p}(\omega)\rangle^{*}, \\
&\langle \delta S_{o_p}(\omega)\delta\phi_q(\omega)\rangle \\
&\quad = H^{p}_{ssi}(\omega){H^{q}_{\phi si}}^{*}(\omega)\langle \delta S_{inj_p}(\omega)\delta S_{inj_q}(\omega)\rangle \\
&\qquad + H^{p}_{s\phi i}(\omega){H^{q}_{\phi\phi i}}^{*}(\omega)\langle \delta\phi_{inj_p}(\omega)\delta\phi_{inj_q}(\omega)\rangle \\
&\qquad + H^{p}_{ssi}(\omega){H^{q}_{\phi\phi i}}^{*}(\omega)\langle \delta S_{inj_p}(\omega)\delta\phi_{inj_q}(\omega)\rangle \\
&\qquad + H^{p}_{s\phi i}(\omega){H^{q}_{\phi si}}^{*}(\omega)\langle \delta S_{inj_q}(\omega)\delta\phi_{inj_p}(\omega)\rangle^{*},
\end{aligned}$$

where the correlation function in the equations above are divided into two categories, $p = q$ and $p \neq q$. When $p = q$, they are already shown in part A of the theoretical mode. If $p \neq q$, the correlation function are derived as

$$\begin{aligned}
\langle \delta S_{inj_p}(\omega)\delta S_{inj_q}(\omega)\rangle &= \frac{S_{inj_p}S_{inj_q}}{P_{inj_p}P_{inj_q}}10^{\frac{Att_p+Att_q}{10}}(1-R)^2 \\
&\quad\times\left(\frac{1}{2}h\nu\upsilon_g\alpha_m V/\Gamma\right)^2\langle|\delta S_m(\omega)|^2\rangle, \\
\langle \delta\phi_{inj_p}(\omega)\delta\phi_{inj_q}(\omega)\rangle &\approx \langle|\delta\phi_m(\omega)|^2\rangle, \\
\langle \delta S_{inj_p}(\omega)\delta\phi_{inj_q}(\omega)\rangle &= \frac{S_{inj_p}}{P_{inj_p}}10^{\frac{Att_p}{10}}(1-R) \\
&\quad\times\left(\frac{1}{2}h\nu\upsilon_g\alpha_m V/\Gamma\right)\langle\delta S_m(\omega)\delta\phi_m(\omega)\rangle.
\end{aligned}$$

The values of other correlation functions not presented are zero.

[1] L. A. Coldren, S. W. Corzine, and M. L. Mashanovitch, *Diode Lasers and Photonic Integrated Circuits* (John Wiley & Sons, New York, 2012), Vol. 218.

[2] B. Xiong, X. Ke, Y. Luo, C. Sun, J. Wang, Z. Hao, Y. Han, L. Wang, and H. Li, *Semiconductor Laser Conference (ISLC), 2016 International* (IEEE, New York, 2016), p. WE37.

[3] J.-S. Huang, H. Lu, and H. Su, *Lasers and Electro-Optics Society, 2008. LEOS 2008. 21st Annual Meeting of the IEEE* (IEEE, New York, 2008), pp. 894–895.

[4] J.-R. Burie, G. Beuchet, M. Mimoun, P. Pagnod-Rossiaux, B. Ligat, J. Bertreux, J.-M. Rousselet, J. Dufour, P. Rougeolle, and F. Laruelle, *Novel In-Plane Semiconductor Lasers IX* (International Society for Optics and Photonics, San Francisco, CA, 2010), Vol. 7616, p. 76160Y.

[5] Y.-G. Zhao, X. Luo, D. Tran, Q. Hang, P. Weber, T. Hang, R. Knust-Graichen, N. Nuttall, R. Cendejas, A. Nikolov *et al.*, *Avionics, Fiber-Optics and Photonics Technology Conference (AVFOP), 2012 IEEE* (IEEE, New York, 2012), pp. 66–67.

[6] M. Faugeron, M. Tran, F. Lelarge, M. Chtioui, Y. Robert, E. Vinet, A. Enard, J. Jacquet, and F. Van Dijk, IEEE Photon. Technol. Lett. **24**, 116 (2012).

[7] A. Capua, L. Rozenfeld, V. Mikhelashvili, G. Eisenstein, M. Kuntz, M. Laemmlin, and D. Bimberg, Opt. Express **15**, 5388 (2007).

[8] G. Baili, L. Morvan, G. Pillet, and S. Bouchoule, J. Lightwave Technol. **32**, 3489 (2015).

[9] N. Girard, G. Baili, P. Nouchi, and D. Dolfi, *International Conference on Group IV Photonics* (IEEE, New York, 2014), pp. 207–208.

[10] L. Chrostowski, C. H. Chang, and C. Chang-Hasnain, *Lasers and Electro-Optics Society, 2003. Leos 2003. The Meeting of the IEEE* (IEEE, New York, 2003), Vol. 2, pp. 706–707.

[11] L. Chrostowski, X. Zhao, and C. J. Chang-Hasnain, IEEE Trans. Microwave Theory Tech. **54**, 788 (2006).

[12] W. Marshall, J. Paslaski, and A. Yariv, Appl. Phys. Lett. **68**, 2496 (1996).

[13] M. C. Soriano, J. Garcíaojalvo, C. R. Mirasso, and I. Fischer, Rev. Mod. Phys. **85**, 421 (2013).

[14] E. K. Lau, L. J. Wong, and M. C. Wu, IEEE J. Sel. Top. Quantum Electron. **15**, 618 (2009).

[15] L. Gillner, G. Björk, and Y. Yamamoto, Phys. Rev. A **41**, 5053 (1990).

[16] G. Yabre, H. De Waardt, H. P. van den Boom, and G.-D. Khoe, IEEE J. Quantum Electron. **36**, 385 (2000).

[17] X. Jin and S.-L. Chuang, Appl. Phys. Lett. **77**, 1250 (2000).

[18] N. Schunk and K. Petermann, IEEE J. Quantum Electron. **22**, 642 (1986).

[19] Y. Yamamoto and N. Imoto, IEEE J. Quantum Electron. **22**, 2032 (1986).

[20] R. Hui, A. D'Ottavi, A. Mecozzi, and P. Spano, IEEE J. Quantum Electron. **27**, 1688 (1991).

[21] P. Spano, S. Piazzolla, and M. Tamburrini, J. Quantum Electron. **22**, 427 (1986).

[22] W. Ma, B. Xiong, X. Ke, C. Sun, Y. Luo, Z. Hao, J. Wang, Y. Han, L. Wang, and H. Li, *Asia Communications and Photonics Conference* (Optical Society of America, Washington, DC, 2017), pp. M1D–4.